

# Crystal Structure of a Preacylation Complex of the $\beta$ -Lactamase Inhibitor Sulbactam Bound to a Sulfenamide Bond-Containing Thiol- $\beta$ -lactamase

Elizabeth A. Rodkey,<sup>†</sup> Sarah M. Drawz,<sup>‡</sup> Jared M. Sampson,<sup>†,#</sup> Christopher R. Bethel,<sup>‡</sup> Robert A. Bonomo,<sup>‡,§,||,⊥</sup> and Focco van den Akker<sup>\*,†</sup>

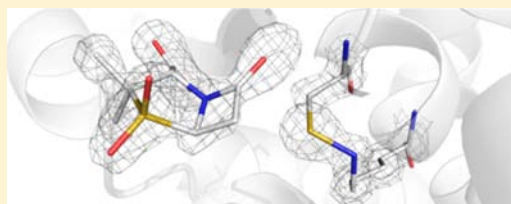
<sup>†</sup>Department of Biochemistry, Case Western Reserve University, 10900 Euclid Avenue, Cleveland, Ohio 44106, United States

<sup>‡</sup>Research Service, Louis Stokes Cleveland Department of Veterans Affairs Medical Center, 10701 East Boulevard, Cleveland, Ohio 44106, United States

<sup>§</sup>Department of Medicine, <sup>||</sup>Pharmacology, and <sup>⊥</sup>Molecular Biology and Microbiology, Case Western Reserve University, 10900 Euclid Avenue, Cleveland, Ohio 44106, United States

## Supporting Information

**ABSTRACT:** The rise of inhibitor-resistant and other  $\beta$ -lactamase variants is generating an interest in developing new  $\beta$ -lactamase inhibitors to complement currently available antibiotics. To gain insight into the chemistry of inhibitor recognition, we determined the crystal structure of the inhibitor preacylation complex of sulbactam, a clinical  $\beta$ -lactamase inhibitor, bound in the active site of the S70C variant of SHV-1  $\beta$ -lactamase, a resistance enzyme that is normally present in *Klebsiella pneumoniae*. The S70C mutation was designed to affect the reactivity of that catalytic residue to allow for capture of the preacylation complex. Unexpectedly, the 1.45 Å resolution inhibitor complex structure revealed that residue C70 is involved in a sulfenamide bond with K73. Such a covalent bond is not present in the wild-type SHV-1 or in an apo S70C structure also determined in this study. This bond likely contributed significantly to obtaining the preacylation complex with sulbactam due to further decreased reactivity toward substrates. The intact sulbactam is positioned in the active site such that its carboxyl moiety interacts with R244, S130, and T235 and its carbonyl moiety is situated in the oxyanion hole. To our knowledge, in addition to being the first preacylation inhibitor  $\beta$ -lactamase complex, this is also the first observation of a sulfenamide bond between a cysteine and lysine in an active site. Not only could our results aid, therefore, structure-based inhibitor design efforts in class A  $\beta$ -lactamases, but the sulfenamide-bond forming approach to yield preacylation complexes could also be applied to other classes of  $\beta$ -lactamases and penicillin-binding proteins with the SXXX motif.



## INTRODUCTION

$\beta$ -Lactam antibiotics inactivate penicillin-binding proteins, thus inhibiting cell wall synthesis, a process that results in bacterial cell death. Bacteria counteract this by producing enzymes called  $\beta$ -lactamases. These enzymes confer antibiotic resistance by hydrolyzing  $\beta$ -lactam antibiotics, such as penicillins and cephalosporins, before they reach their intended target.<sup>1</sup> To combat this resistance mechanism,  $\beta$ -lactams are often administered with  $\beta$ -lactamase inhibitors.<sup>2</sup> Unfortunately, new inhibitor-resistant  $\beta$ -lactamase variants arose in the clinic that were resistant to currently available inhibitors, particularly clavulanic acid. As these resistant enzymes threaten antibiotic potency, development of novel inhibitors is one strategy to ensure continued antibiotic efficacy.<sup>3</sup>

Currently, there are three  $\beta$ -lactamase inhibitors available for clinical use: sulbactam, clavulanic acid, and tazobactam (Figure 1A–C). These inhibitors function by a similar serine-acylation mechanism summarized here for sulbactam (Supporting Information Figure S1, similar to tazobactam<sup>4</sup>). Upon preacylation complex formation (species 2), a tetrahedral intermediate is formed at the catalytic S70 residue (species 3).

The  $\beta$ -lactam ring is broken forming the acyl intermediate (species 4), followed by breakage of the C–S bond thereby forming an imine intermediate (species 6). The more reactive imine species (species 6) leads to either: irreversible inhibition, regeneration of active enzyme, or transient inhibition. Irreversible inhibition may occur as a result of covalent modification by serine 130 and is likely an infrequently traveled arm of the pathway as is evidenced by both high turnover numbers for several common enzymes (reviewed in ref 5) and unaffected partition ratio in the S130G variant.<sup>6</sup> Regeneration of active enzyme occurs via deacylation by a nearby activated water molecule primed by E166 and N170; this completes the reaction and frees the active site of the inhibitor. Transient inhibition occurs when the imine species tautomerizes to the *cis*- (species 5) or *trans*-enamine (species 7) species. The *trans*-species (species 7) is a potentially energetically favorable intermediate and the relatively short doubling time of bacteria could allow for a long-lived *trans*-enamine species to be an

Received: July 26, 2012

Published: September 13, 2012

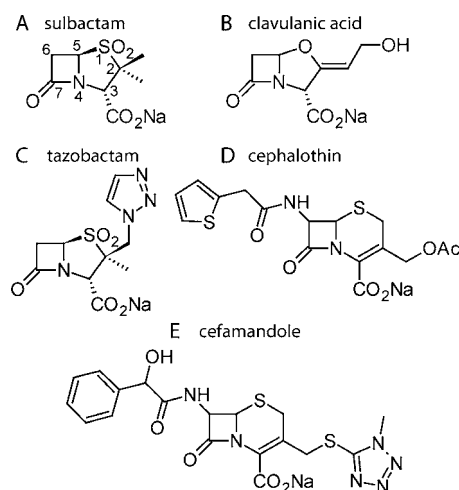


**Figure 1.** Chemical structures of three clinically available inhibitors: (A) sulbactam, (B) clavulanic acid, (C) tazobactam and two substrates: (D) cephalothin, (E) cefamandole.

effective inhibition strategy. A number of inhibitor intermediates have been crystallographically captured such as the *trans*- and *cis*-enamine,<sup>4,7–10</sup> imine,<sup>11</sup> acylation transition state<sup>12,13</sup> and deacylation transition state.<sup>13–15</sup> However, the structure of a preacylation/Michaelis–Menten complex is one inhibitor complex that has yet to be determined. In efforts to aid structure-based design of new inhibitors, knowledge of detailed inhibitor interactions in the active site prior to acylation would be beneficial. Such a complex would allow delineation of which interactions may be critical for initial inhibitor recognition and affinity. However, crystallographic trapping of the preacylation complex is not trivial as the acylation step occurs rapidly in the wild-type (*wt*) enzyme. Therefore, a strategic approach would be to slow down the acylation rate to an extent that would allow for capture of the noncovalent inhibitor–enzyme complex. Previously, two other groups have succeeded in obtaining preacylation complexes of substrates by specific site-directed mutagenesis. The first study examined a S64G (equivalent to S70G in sulphydryl variable (SHV-1)) AmpC  $\beta$ -lactamase variant in complex with a first-generation cephalosporin, cephalothin (Figure 1D).<sup>16</sup> A second study used a K73A substitution to capture a preacylation complex between a second-generation cephalosporin, cefamandole (Figure 1E), and the  $\beta$ -lactamase BlaC.<sup>17</sup> These structures captured preacylation complexes of substrates, not of  $\beta$ -lactamase inhibitors. As neither of the two mutant variant approaches was successful for SHV-1  $\beta$ -lactamase enzyme, we generated a different active site mutant in which the catalytic serine is substituted by a cysteine (S70C). Compared to oxygen, the radius of sulfur of the cysteine is larger and is less electronegatively charged; these differences were explored, as one of the strategies in the lab, to crystallographically capture a preacylation complex. S70C thiol- $\beta$ -lactamase was first described in 1982 by Sigal et al.<sup>18</sup> and was found to have greatly reduced resistance to ampicillin as evidenced by dramatically decreased  $k_{\text{cat}}$  values, as compared to *wt* TEM enzyme.<sup>19</sup> The thiol-introducing mutation in SHV-1 allowed successful trapping of the desired Michaelis–Menten inhibitor complex. Herein, we present the crystal structure of the preacylation complex between S70C thiol- $\beta$ -lactamase and the inhibitor sulbactam. Our results provide insights into the early steps of the inactivation mechanism by a sulfone inhibitor.

## MATERIALS AND METHODS

**Expression and Purification.** To improve expression yield, the SHV-1 gene was subcloned without leader sequence into pET24a+ (Novagen) from an SHV-1 pBC SK- construct described previously.<sup>20</sup> *bla*<sub>SHV-1</sub> was first amplified with primers containing 5' NdeI and 3' BamHI sites. Serine 70 to cysteine mutagenesis was performed using QuikChange Site-Directed Mutagenesis kit (Stratagene). Mutagenized DNA was transformed into OneShot BL21 Star (DE3) Chemically Competent *Escherichia coli* cells (Invitrogen) and plated on a 50  $\mu\text{g}/\text{mL}$  kanamycin lysogeny broth (LB) agar plate. Plated cells were used to inoculate larger LB cultures; details can be found in Supporting Information. The protein was purified by preparative isoelectric focusing (pIEF) (See Supporting Information text for details) followed by gel filtration using a Superdex 75 column (GE LifeSciences). Purified protein was concentrated to 5 mg/mL using a 10K MWCO centrifugal concentrator (Amicon).

*wt*SHV-1 protein was also expressed and purified, as we wanted a higher resolution structure than was currently available (PDB ID: 1SHV at 1.98 Å) to make detailed comparisons to the S70C structures. The *wt* protein was expressed in a pBC SK(-) vector in *E. coli* DH10B cells (Stratagene). Cells were grown overnight in LB supplemented with 20  $\mu\text{g}/\text{mL}$  chloramphenicol. Cells were lysed with stringent periplasmic fractionation and the protein was purified as described above. *wt*SHV-1 was also concentrated to 5 mg/mL.

**Crystallization and Soaking.** *wt*SHV-1 and S70C crystals were grown using the vapor diffusion method in 24-well sitting drop trays (Hampton Research) using a 500  $\mu\text{L}$  reservoir solution of 21–30% PEG6000 and 0.1 M HEPES pH 6.8–7.8. A total of 5 mg/mL protein was combined with Cymal-6 (final concentration 0.56 mM, Hampton Research) then mixed with the reservoir solution at a 1:1 ratio to a final drop size of 5  $\mu\text{L}$ . Inhibitor soaks of S70C crystals were performed in well solution plus 50 mM sulbactam for 1 min. Crystals were subsequently cryoprotected in well solution supplemented with 20% 2-methyl-2,4-pentandiol (well solution for inhibitor soaked S70C crystals also contained 50 mM sulbactam) prior to immersion in liquid nitrogen.

**Data Collection and Refinement.** X-ray diffraction data was collected on a MAR-325 CCD detector at the Stanford Synchrotron Radiation LightSource (SSRL) beamline BL9-2. Images were integrated and scaled using HKL2000.<sup>21</sup> *wt* and S70C crystallize in space group  $P2_12_12_1$  (see Supporting Information Table S1 for more statistics). The structures were determined by isomorphous replacement using an apo *wt*SHV-1 structure (PDB ID: 1SHV). Restrained isotropic (apo S70C and S70C:sulbactam complex) and restrained anisotropic (*wt*SHV-1) refinements were performed using Refmac5 in the CCP4 suite.<sup>22</sup> Model building and manual refinement were carried out using COOT.<sup>23</sup> A total of 98.09% of residues fell in Ramachandran preferred regions, 1.15% in allowed regions and 0.76% in outlying regions. Upon refinement, an unreacted sulbactam molecule was observed in the active site of S70C (Figures 2 and 3). Sulbactam was subsequently included in refinement. A sulbactam topology file was generated using the online PRODRG2 server.<sup>24</sup> The coordinates of the *wt*SHV-1, apo S70C, and S70C:sulbactam complex were deposited at the Protein Data Bank and the PDB IDs are 4FH4, 4FD8, and 4FH2, respectively.

**Kinetics.** The steady-state kinetic constants of the *wt*SHV-1 and S70C  $\beta$ -lactamases were determined by continuous assays at room temperature with a model 8452 diode array spectrophotometer (Agilent). Each assay was performed in 10 mM phosphate-buffered saline (PBS) at pH 7.4.  $V_{\text{max}}$  and  $K_{\text{m}}$  were obtained by measuring the hydrolysis of nitrocefirin (NCF) (BD Biosciences, San Jose, CA) ( $\Delta\epsilon_{482} = 17\,400\ \text{M}^{-1}\ \text{cm}^{-1}$ ) and obtaining the nonlinear least-squares fit of the data to the Henri–Michaelis–Menten equation by using the program Enzfitter (Biosoft Corporation):

$$v = (V_{\text{max}} \times [S]) / (K_{\text{m}} + [S])$$

Here,  $v$  is the initial rate of hydrolysis and  $[S]$  is the substrate concentration.

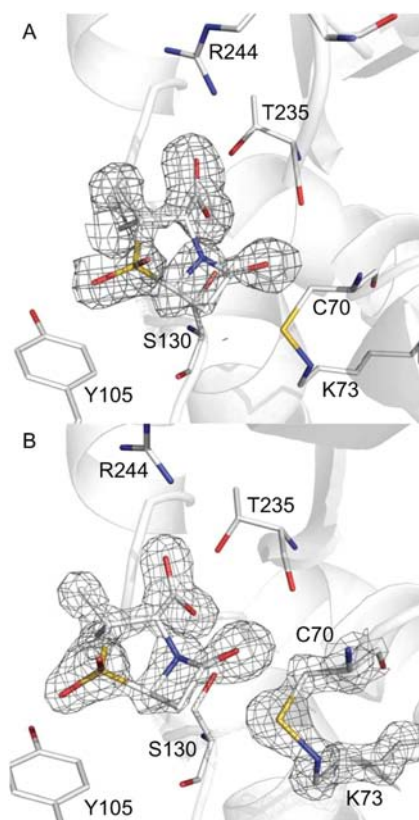


**Figure 2.** Intact, unreacted sulbactam in the S70C active site. (A)  $F_o - F_c$  density contoured at  $2.75\sigma$ ; (B)  $2F_o - F_c$  density contoured at  $1.0\sigma$ .

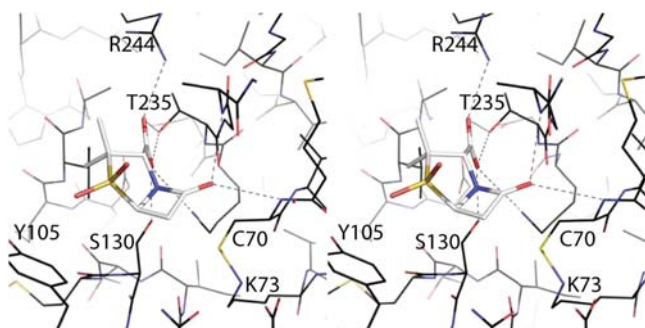


**Figure 3.** Stereo figure depicting sulbactam in the active site of S70C.

## RESULTS

The crystal structure of S70C thiol- $\beta$ -lactamase soaked with sulbactam yielded a nonreacted sulbactam molecule in the active site (Figures 2 and 3) which will be discussed below. First, the S70C mutation in SHV did not result in large structural changes as compared to *wt*SHV-1: an all- $\alpha$  superpositioning resulted in a relatively low root mean squared deviation (rmsd) of 0.31 Å. There were, however, a couple of intriguing differences within the S70C protein structure as compared to the *wt*SHV-1 structure. Firstly, in the S70C mutant structure the intramolecular disulfide bond was absent. In *wt*SHV-1, an intramolecular disulfide bond was formed between cysteine residues 77 and 123, but in the S70C mutant, this bond was reduced (Supporting Information Figure S2A,B), likely a consequence of the adapted nonperiplasmic expression procedure. Despite the loss of the disulfide in the S70C mutant, the folding of the protein was not affected, as was evident by

the low overall rmsd mentioned above and by the fact that the enzyme remained partially active despite having the catalytic residue mutated. In fact, the hydrolytic rate (turnover number) was relatively preserved; our kinetic experiments indicated that the change in catalytic efficiency was primarily a result of an increase in  $K_m$ .

A second, and unexpected, feature of the S70C structure was the presence of a sulfenamide linkage in the active site (Figure 2B and Supporting Information Figure S2D) which has not previously been described in the thiol- $\beta$ -lactamase.<sup>18,19</sup> The sulfur of C70 and nitrogen of the K73 side chains formed a covalent linkage, termed a sulfenamide, with strong continuous electron density between the two side chains that was absent in the *wt* structure (Supporting Information Figure S2D,E). C70 and, to a greater extent, K73, moved toward one another to create the covalent bond. Although we collected several soaked S70C data sets that had clear, fully formed sulfenamide bonds, the degree to which the sulfenamide bond was formed was different among all of the S70C data sets collected. The crystallographic observations regarding the sulfenamide bond ranged from fully formed, fully formed with two different sulfenamide bond geometries (not shown), to unformed in  $\sim 15$  data sets. For comparison, we included here the structure of apo S70C (Figure 4) which did not have a sulfenamide bond

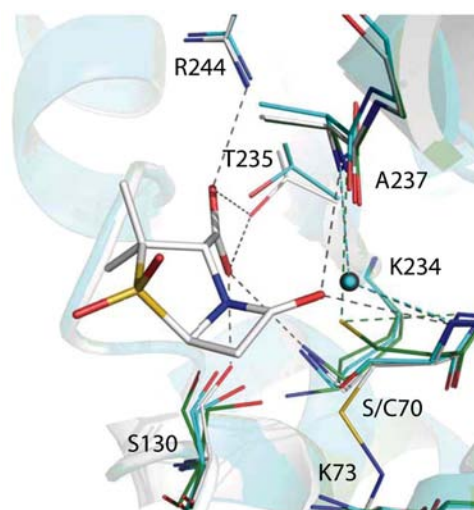


**Figure 4.** Superposition of S70C:sulbactam (gray), apo S70C (green) and apo *wt*SHV-1 (cyan). Shown are residues within hydrogen bonding distance of the carboxylic acid group of sulbactam, multiple conformations for S130 and K234 and similarity of R244 and T235 conformations across the three structures. Also depicted are oxanyon hole occupants: partially occupied water molecules in the apo *wt*SHV-1 (cyan sphere) and S70C:sulbactam (gray sphere, mostly eclipsed by cyan sphere) structures and lack of water in apo S70C structure because C70 sulfur has shifted toward that position. Superpositions were performed using SSM Superpose utility in COOT.<sup>45</sup>

in the active site (Supporting Information Figure S2F). When we compared this structure to the S70C:sulbactam structure, we observed that C70 and K73 side chains shift 2.2 and 1.9 Å, respectively (Figure 4). Other conformational differences were seen for residues S130 and K234. In the apo S70C structure, these residues have two conformations; in the preacylation complex structure, these residues have a single orientation (Figure 4). The rest of the active site, including residues 166, 235, 237, and 244 had not shifted significantly (Figure 4).

Despite the absence of the original disulfide bond and the unexpected presence of the sulfenamide linkage in the sulbactam complex, the S70C:sulbactam and *wtSHV-1* active sites are very similar. The positions of most key active site residues in the mutant enzyme shifted less than 1 Å as compared to the *wt* enzyme (Ambler positions 70, 130, 234, and 244 with the exception of 70 and 73; Figure 4). An all-atom superposition of the S70C and *wtSHV-1* active site residues within 10 Å resulted in an rmsd of 0.375 Å. Therefore, even with the changes in residue 70 and 73 positioning; the mutant active site retained a very similar structure to that of the *wt* enzyme, such that one anticipates little change in how the inhibitor approaches the active site.

Soaking sulbactam into S70C crystals allowed for the capture of the preacylation complex between the inhibitor and the mutant enzyme (Supporting Information Table S1, Figures 2 and 3). With the residue at position 70 being involved in a covalent bond, C70 is likely not as reactive toward substrates/inhibitors; this probably contributed toward obtaining the previously unattainable preacylation inhibitor complex. This structure represents, to our knowledge, the first preacylation complex between a  $\beta$ -lactamase enzyme and an inhibitor. Clear density was present for the entire intact sulbactam species situated in the active site (Figure 2A,B). Strong bifurcated density representing the carboxylic acid moiety as well as strong density for the carbonyl oxygen that occupied the oxyanion hole were observed. Strong density was also observed for sulbactam's dimethyl sulfone moiety. Density for the four-membered  $\beta$ -lactam ring was slightly weaker but still present in an unbiased omit electron density map contoured at  $2.75\sigma$ . Sulbactam was refined with an occupancy of 75% because refinement with occupancy of 100% resulted in the appearance of some negative density. When we inspected the active site interactions between inhibitor and enzyme we observed that the inhibitor carbonyl was in close proximity to the oxyanion hole formed by the backbone nitrogens of S70 and A237 (Figures 3 and 4). In addition, the carboxylic acid moiety was within hydrogen bonding distance of R244, S130, T235 and, weakly, to K234 (Figures 3 and 4). The carbonyl-oxyanion hole interactions and the latter three carboxylic acid interactions were predicted in previous modeling experiments.<sup>25</sup>

In addition to a 75% occupied sulbactam, we also included a 25% occupancy water (gray sphere; Figure 4) in the oxyanion hole of the S70C:sulbactam structure, located essentially where the oxyanion hole water is located in the apo *wtSHV-1* structure (cyan sphere). Moreover, the carbonyl oxygen of sulbactam was positioned very near to the oxyanion hole. Interestingly, the C70 sulfur in the apo S70C structure was also approaching the oxyanion hole, after having shifted 2.2 Å from its sulfenamide bond forming position in the S70C:sulbactam complex structure and 1.6 Å from its oxygen position in the apo *wtSHV-1* structure (Figure 4). The sulfur was in closer proximity to the oxyanion hole in the apo S70C structure, likely as a consequence of the larger radius of the sulfur; therefore, unlike in the *wtSHV-1* structure, there was no oxyanion water observed in the apo S70C structure.

The steady state kinetics of the S70C enzyme were assessed using nitrocefin. The  $K_m$  of the mutant for nitrocefin ( $1260 \pm 10 \mu\text{M}$ ) was more than 250-fold greater than for the *wtSHV-1*  $\beta$ -lactamase ( $5 \pm 0.9 \mu\text{M}$ ).<sup>6</sup> This may be a result of the altered charge in the active site environment of the S70C mutant. While the  $k_{\text{cat}}$  values for the two enzymes were comparable (*wtSHV-1*,  $142 \pm 4 \text{ s}^{-1}$ , and S70C,  $111.05 \pm 11.10 \text{ s}^{-1}$ ), the

large difference in  $K_m$  resulted in a significant drop in catalytic efficiency (*wtSHV-1*  $k_{\text{cat}}/K_m = 28.4 \pm 4.3 \mu\text{M}^{-1} \text{ s}^{-1}$ ,<sup>6</sup>; S70C  $k_{\text{cat}}/K_m = 0.0881 \mu\text{M}^{-1} \text{ s}^{-1}$ ).

## DISCUSSION

In this study, we determined the structure of the preacylation complex between a mutant SHV-1  $\beta$ -lactamase and an inhibitor. Specifically, we delineated which interactions are important in initial inhibitor binding as this information could aid in the design of an inhibitor which would potentially have enhanced preacylation complex interactions, higher binding affinity, and/or a broader spectrum of inhibition.

**S70C versus *wtSHV-1*.** Our use of a S70C mutant to capture the preacylation complexes is novel. As previously shown, the S70C mutant in TEM-1 did not disrupt the overall structure; nearly identical circular dichroism measurements were seen between their thiol- $\beta$ -lactamase and the *wt* enzyme, indicating that the mutant is similarly folded as compared to the *wt*.<sup>19</sup> In agreement, we observed a nearly identical global structure in S70C and *wtSHV-1* ( $C\alpha$  rmsd of 0.31 Å). Note that in order to improve expression yields, S70C was expressed in the cytoplasm without export to the periplasm as the leader sequence had been deleted from the construct. As a result, the C77–C123 disulfide bond is not formed in the S70C protein (Supporting Information Figure S2A,C). The similarity of the *wt* and mutant protein structures indicates that the lack of the disulfide bond did not significantly affect the overall structure. In addition, this disulfide bond is likely not critical for catalytic activity as studies of a TEM-1 C77S mutant found that the biphasic folding time course of the enzyme was not significantly affected by the mutation and that the mutant enzyme retained enzymatic activity despite a decrease in thermal stabilization.<sup>26</sup> We believe that sulbactam is bound in the active site in a close-to-productive mode, as the extrapolated S70 oxygen position is at good distance (2.49 Å) for nucleophilic attack of the carbonyl carbon with the carbonyl oxygen situated in the oxyanion hole. This is evidenced by comparison of the S70C structure to that of the SHV-sulbactam acyl enzyme structure (PDB ID: 2A3U)<sup>7</sup> as detailed in the Supporting Information. Note that the oxyanion hole holding the carbonyl oxygen likely serves the purpose of making the carbonyl carbon more susceptible, via partial charge redistribution, to nucleophilic attack during the acylation reaction (by S70) and deacylation reaction (by the deacylation water).

**Kinetic Analysis.** Although the S70C and *wtSHV-1* enzymes are very similar when the overall structures are compared, their ability to hydrolyze nitrocefin differs. The  $K_m$  of nitrocefin for S70C is approximately 250-fold larger than that of *wt*; in contrast, the  $k_{\text{cat}}$  is slightly lower. The large difference in  $K_m$  results in a greatly reduced catalytic efficiency as reflected by the 310-fold lower  $k_{\text{cat}}/K_m$  ratio. The same trend (large increase in  $K_m$ , decreased  $k_{\text{cat}}$ , and greatly reduced  $k_{\text{cat}}/K_m$ ) is also seen in the TEM thiol- $\beta$ -lactamase<sup>19</sup> and in inhibitor resistant mutants.<sup>6</sup> Our kinetic data supports the crystallographic observation that the active site structure is largely unchanged in the S70C mutant, thus preserving hydrolytic rate ( $k_{\text{cat}}$ ) despite substitution of the active site serine.

We advance that the alterations in the active site partial charges and/or increased radius of the sulfur atom result in a  $K_m$  of nitrocefin that is significantly higher for the mutant. Overall, the kinetic data suggest that the rate constants that govern the initial steps in recognition and formation of the covalent complex are impaired. However, once nitrocefin is

positioned in the active site, hydrolysis proceeds at a similar rate as in the *wt* enzyme. Alternatively, binding could be more rate-limiting in the mutant, in which case  $K_m$  may not equal  $K_D$ . We stress that the status of the sulfenamide linkage in the protein used for these kinetic assays is unknown. We anticipate that the C70–K73 sulfenamide is likely not formed in solution as both residues 70 and 73 have previously been shown to be important for acylation.<sup>27</sup> Future studies with additional substrates will provide insight into the general nature of these hypotheses.

**Sulbactam Active Site Interactions.** As mentioned above, sulbactam interacts with the active site at the oxyanion hole via the carbonyl moiety and with residues R244, S130, K234 and T235 via its carboxylic acid moiety (Figures 3 and 4). These observed interactions are in agreement with previous studies.<sup>25,28,29</sup> Interestingly, all but T235 have been found to be substituted in SHV and/or TEM inhibitor resistant variants (S130G,<sup>30,31</sup> K234R,<sup>32</sup> and R244S/C<sup>33</sup>) indicating that these interactions are indeed critical for inhibitor recognition and activity. We have used S70C in an attempt to capture preacylation complexes of an additional 14 inhibitors, including tazobactam and clavulanic acid, but were unsuccessful. However, based on the position of sulbactam in the active site, we can extrapolate the position of the clavulanic acid and tazobactam C2 moieties. The C2 methyl groups of sulbactam in the S70C complex structure are oriented away from the active site, into the solvent. As such, one could assume the longer C2 moieties of the other two inhibitors would occupy a similar location. Such a position would potentially allow for the clavulanic acid hydroxyethylidene and tazobactam triazole moieties to be within van der Waals distance of R244 and M272. Future studies need to be carried out to determine whether such hypothesized interactions indeed occur. The preacylation complex structure also yields clues as to how to further improve sulbactam to increase interactions formed in the preacylation complex. There is ample space near the methyl groups at the C2 position such that changing those moieties into longer chemical substituents could potentially lead to additional interactions in the active site. If chemically feasible, even the oxygens on the sulfone moiety of sulbactam could be used to connect additional chemical moieties to increase active site interactions.

**Comparison to Preacylation Substrate–Enzyme Complexes.** As this is the first crystallographic description of a preacylation complex between a  $\beta$ -lactamase and an inhibitor, we can now compare this complex to previously determined preacylation substrate–enzyme complexes. When comparing the S70C:sulbactam structure to that of the AmpC-cephalothin (PDB ID: 1KVL) structure, we find the interactions are similar between the two structures (Figure 5A). Residues are mentioned for SHV followed by AmpC. First, the carbonyl oxygen in both structures is situated in the oxyanion hole. Also, both the substrate and inhibitor share a hydrogen bond with S130/Y150 (2.5 and 3.2 Å, respectively) as well as generate a salt bridge with K234/K315, although the latter distance is substantially larger in the sulbactam complex (3.9 and 3.3 Å, respectively). Cephalothin thus makes a stronger interaction with K315 than sulbactam does with K234. More significant differences are seen near R244/N346 where the bond distance between the carboxylic acid moiety of sulbactam and the respective amino acids is increased by about 80% (2.82 to 5.17 Å) in the AmpC structure. The effective loss of this hydrogen bond is compensated for by water-mediated hydrogen bonds to

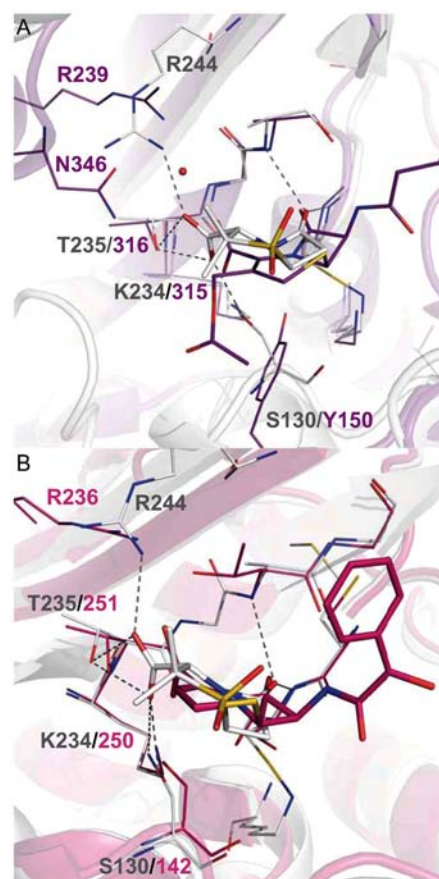


**Figure 5.** Substrate preacylation complex superpositions show similarities and discrepancies in active site interactions: (A) S70C:sulbactam (gray) and AmpC:cephalothin (purple, 1KVL). Residues 69–73, 132, and 234–238 were aligned with residues 63–67, 152, and 315–219, respectively. (B) S70C:sulbactam (gray) and BlaC:cefamandole (pink, 3NY4). Residues 69–73, 132, and 234–238 were aligned with residues 83–87, 144, and 250–254, respectively. Superpositions were performed using the LSQKAB program in the CCP4 suite<sup>46</sup>.

R349 and N346 (Figure 5A). Differences are expected between the active sites of class A (S70C) and class C (AmpC) enzymes and these discrepancies highlight the adaptability of the active sites and their ability to perform the same function.<sup>34</sup>

The second structural comparison involves the BlaC-cefamandole substrate preacylation structure (PDB ID: 3NY4)<sup>17</sup> and the S70C:sulbactam structure. The ligand interactions are relatively similar, which might be expected as both are class A enzymes. In both structures, the carbonyl oxygen is in the oxyanion hole (Figure 5B). In addition, the carboxylic acid group is able to make four conserved contacts: S130/142, T235/251, R244/220, and K234/250 (for SHV and BlaC, respectively). Note that R244 is missing in BlaC but R220 assumes this role with its guanidinium group in a different orientation but similar location. A fifth contact is seen in the BlaC structure as T253 is within hydrogen bonding distance (2.3 Å) of the cefamandole carboxylic acid group.<sup>17</sup> This contact is missing in the S70C structure as this residue is an alanine (Figure 5B).

In SHV, inhibitor-resistant mutations are known to affect substrate and inhibitor affinity to different degrees.<sup>5,6,35</sup> Although many structural similarities exist between the inhibitor and substrate preacylation complexes, some subtle

differences could yield insights into how the inhibitor resistant mutations affect substrate and inhibitor efficacies. The structural comparisons described above indicate that the inhibitor forms a shorter (2.8 Å), and presumably tighter, hydrogen bond to R244 than substrates do to the synonymous residues (3.5 Å). R244S SHV was found to have 63 times higher  $K_i$  and 28 times lower inhibition efficiency ( $k_{\text{inact}}/K_i$ ) toward clavulanic acid. In contrast,  $k_{\text{cat}}/K_m$  of ampicillin was lowered by only 14 times and  $K_m$  increased by only 1.5 times by this mutation.<sup>35</sup> On the other hand, these comparisons show that the inhibitor and substrate make hydrogen bonds of similar length (2.5 and 2.4 Å) to S130 (and homologous residues). S130G was found to have 332 times higher  $K_i$  and 420 times lower inhibition efficiency for clavulanic acid. The catalytic efficiency and  $K_m$  for the substrate ampicillin were affected to a greater extent than was seen in R244S, with an increase in  $K_m$  of 2.3-fold and catalytic efficiency of 28 times.<sup>6</sup> These observations suggest that the proximity with which the ligand forms hydrogen bonds with the enzyme may be an important factor when considering affinity and inhibition efficiency. Note that changes in other inhibitor interactions during subsequent inhibition steps, such as deacylation, could also account for the observed kinetic differences.

**S70C Sulfenamide Formation and Implications for  $\beta$ -Lactamase Acylation.** The observation of a covalent bond between C70 and K73 was unexpected, yet, although rare, sulfenamide bonds have been observed and utilized before in other systems as discussed in Supporting Information Text. Cyclic sulfenamides were first described in protein tyrosine phosphatase 1B (PTP1B) with regard to redox regulation.<sup>36,37</sup> PTP1B is further discussed in Supporting Information. While not physiologically relevant in our system, a similar bond formation mechanism may be at work. Salmeen et al. suggested a condensation mechanism for sulfenamide formation, where the cysteine thiol is first oxidized to sulfenic acid. The sulfur, which is partially positively charged, is then attacked by the nucleophilic nitrogen, releasing water and forming the covalent bond.<sup>36</sup> The mechanism for the formation of the sulfenamide in S70C is hypothesized to begin with the conversion of thiol (-SH) to sulfenic acid (-SOH) (Supporting Information Figure S3). Although the sulfenamide in the S70C structure is not formed with a backbone nitrogen but a primary amine nitrogen, it is possible that a similar mechanism is responsible for its formation. In S70C, the reason for C70 oxidation is unclear, but could have taken place during protein expression by reactive oxygen species (e.g.,  $\text{H}_2\text{O}_2$ ) present in the cytoplasm, which would be able to act upon these solvent exposed residues. Alternatively, the oxidation might have occurred in the crystal, where atmospheric oxidants could have acted upon it, or could be due to the reduced disulfide catalyzing the two-electron oxidation reaction to form the sulfenamide bond. Another explanation could stem from the fact that the sulfenamide bond chemistry observed in our structure involves residues primed for catalysis. These residues likely have their  $\text{p}K_a$  modulated for their catalytic roles<sup>38–40</sup> and as such could be more reactive once S70 had been mutated to a cysteine. Note that for further studies, it would be interesting to probe the S70C mutant in the presence of a K73A mutant, as well as the K73A alone, to both kinetically and structurally investigate the relative importance and interactions of the 70 and 73 residues via kinetic and crystallographic experiments (although we anticipate the activity of the double mutant to be very low based as mutating residue K73 caused a drastic decrease in activity<sup>17</sup>). Finally, the

sulfenamide bond formation could have been formed in a substrate-assisted manner as will be detailed in the next paragraph.

Our structure also sheds light on the contentious subject of K73 participation in the acylation half-reaction. Many studies attempt to define the protonation state of K73, yet it remains unclear. There are structures in favor of protonated<sup>41</sup> and unprotonated<sup>42</sup> K73 and at 1.5 Å resolution; our apo S70C and S70C:sulbactam structures cannot definitively reveal the K73 protonation state. However, the only way for the sulfenamide bond formation to occur is through reaction of C70 with a deprotonated K73. It has been shown that, in TEM-1, the active site lysine has a lower  $\text{p}K_a$  (~8.0–8.5) than the other 10 lysines ( $\text{p}K_a$  values ~10–11) because of its proximity to K234 and, to lesser extent, E166.<sup>43</sup> The same study concluded that K73 is protonated at ground-state (unbound) and is unprotonated upon preacylation complex formation.<sup>43</sup> Another analysis attempts to explain the complex proton transfer events in TEM-1 and also found evidence for a protonation status change during the preacylation complex formation step.<sup>44</sup> Their proposed proton transfer scheme also explains the ability of E166A mutants to form acyl-enzymes,<sup>7,17</sup> which has been advanced as support for a deprotonated K73 acylation mechanism. Because the sulfenamide bond is absent in several of our apoS70C structures, our S70C:sulbactam structure offers further support of a K73 acylation mechanism where K73 is protonated in the absence of inhibitor and becomes unprotonated during preacylation complex formation.

As mentioned above, we observed a large variation of sulfenamide bonds in the many data sets collected for this mutant using crystals soaked with inhibitors and substrates or nonsoaked. We do not know what causes the variation among data sets but the possible lability of the sulfenamide bond is in accordance with the reversibility of the bond described in the PTP1B structures.<sup>36,37</sup> The variation could result from a mechanism involving substrate/inhibitor-assisted sulfenamide bond formation where perhaps this bond is formed during the deacylation of the first substrate/inhibitor. Alternatively, variation in sulfenamide bond formation, and in turn K73 protonation state, could result from the fluctuation of sulbactam active-site occupancy, which is inherent in the crystal soaking method. Future studies are needed to investigate these possibilities.

**Conclusions.** Previous studies provided crystal structures of many of the  $\beta$ -lactamase inhibitor intermediates; however, the preacylation complex remained elusive. Here, for the first time, we present the preacylation complex between the inhibitor sulbactam and  $\beta$ -lactamase S70C. This complex provides insight into the interactions occurring prior to acylation. In addition, information gleaned from the comparison of the inhibitor and substrate preacylation complexes sheds light on the differences in their binding modes. These observations could potentially be used for structural-based design of novel, more potent inhibitors to facilitate additional inhibitor–enzyme interactions, to preserve critical interactions, or to circumvent inhibitor–resistant mutations. Such compounds will be important to the future development of sulfone inhibitors because increasing numbers of  $\beta$ -lactamases exhibit inhibitor resistance, in particular clavulanic acid resistance. Finally, because the sulfenamide bond between residues S70C and K73 appears to have contributed to successfully obtaining a preacylation complex, such an approach could be similarly

successful for other classes of serine  $\beta$ -lactamases and penicillin-binding proteins that have the SXXK motif.

## ■ ASSOCIATED CONTENT

### ● Supporting Information

Detailed protein expression and purification methods; an extended discussion of structural comparisons, sulfenamide bonds and PTP1B; Figures S1–S3 and Table S1. This material is available free of charge via the Internet at <http://pubs.acs.org>.

## ■ AUTHOR INFORMATION

### Corresponding Author

focco.vandenakker@case.edu

### Present Address

#Department of Biochemistry and Molecular Pharmacology, New York University School of Medicine, 550 First Ave., New York, NY 10016

### Notes

The authors declare no competing financial interest.

## ■ ACKNOWLEDGMENTS

The following funding sources are acknowledged: NIH (R01 AI062968 to F.v.d.A.; R01 AI063517 to R.A.B.), U.S. Department of Veterans Affairs, Merit Review Program (to R.A.B.), and Cleveland Geriatric Research Education and Clinical Center (to R.A.B.). We thank beamline personnel at SSRL for facilitating data collection.

## ■ REFERENCES

- (1) Essack, S. Y. *Pharm. Res.* **2001**, *18*, 1391–1399.
- (2) Miller, L. A.; Ratnam, K.; Payne, D. J. *Curr. Opin. Pharmacol.* **2001**, *1*, 451–458.
- (3) Bush, K.; Macielag, M. J. *Expert Opin. Ther. Pat.* **2010**, *20*, 1277–1293.
- (4) Totir, M. A.; Padayatti, P. S.; Helfand, M. S.; Carey, M. P.; Bonomo, R. A.; Carey, P. R.; van den Akker, F. *Biochemistry* **2006**, *45*, 11895–11904.
- (5) Drawz, S. M.; Bonomo, R. A. *Clin. Microbiol. Rev.* **2010**, *23*, 160–201.
- (6) Helfand, M. S.; Bethel, C. R.; Hujer, A. M.; Hujer, K. M.; Anderson, V. E.; Bonomo, R. A. *J. Biol. Chem.* **2003**, *278*, 52724–52729.
- (7) Padayatti, P. S.; Helfand, M. S.; Totir, M. A.; Carey, M. P.; Carey, P. R.; Bonomo, R. A.; van den Akker, F. *J. Biol. Chem.* **2005**, *280*, 34900–34907.
- (8) Padayatti, P. S.; Helfand, M. S.; Totir, M. A.; Carey, M. P.; Hujer, A. M.; Carey, P. R.; Bonomo, R. A.; van den Akker, F. *Biochemistry* **2004**, *43*, 843–848.
- (9) Padayatti, P. S.; Sheri, A.; Totir, M. A.; Helfand, M. S.; Carey, M. P.; Anderson, V. E.; Carey, P. R.; Bethel, C. R.; Bonomo, R. A.; Buynak, J. D.; van den Akker, F. *J. Am. Chem. Soc.* **2006**, *128*, 13235–13242.
- (10) Chen, C. C.; Herzberg, O. *J. Mol. Biol.* **1992**, *224*, 1103–1113.
- (11) Kuzin, A. P.; Nukaga, M.; Nukaga, Y.; Hujer, A.; Bonomo, R. A.; Knox, J. R. *Biochemistry* **2001**, *40*, 1861–1866.
- (12) Chen, Y.; Shoichet, B.; Bonnet, R. *J. Am. Chem. Soc.* **2005**, *127*, 5423–5434.
- (13) Wang, X.; Minasov, G.; Blazquez, J.; Caselli, E.; Prati, F.; Shoichet, B. K. *Biochemistry* **2003**, *42*, 8434–8444.
- (14) Ke, W.; Sampson, J. M.; Ori, C.; Prati, F.; Drawz, S. M.; Bethel, C. R.; Bonomo, R. A.; van den Akker, F. *Antimicrob. Agents Chemother.* **2011**, *55*, 174–183.
- (15) Caselli, E.; Powers, R. A.; Blaszczak, L. C.; Wu, C. Y.; Prati, F.; Shoichet, B. K. *Chem. Biol.* **2001**, *8*, 17–31.
- (16) Beadle, B. M.; Trehan, I.; Focia, P. J.; Shoichet, B. K. *Structure* **2002**, *10*, 413–424.
- (17) Tremblay, L. W.; Xu, H.; Blanchard, J. S. *Biochemistry* **2010**, *49*, 9685–9687.
- (18) Sigal, I. S.; Harwood, B. G.; Arentzen, R. *Proc. Natl. Acad. Sci. U.S.A.* **1982**, *79*, 7157–7160.
- (19) Sigal, I. S.; DeGrado, W. F.; Thomas, B. J.; Petteway, S. R. *J. Biol. Chem.* **1984**, *259*, 5327–5332.
- (20) Rice, L. B.; Carias, L. L.; Hujer, A. M.; Bonafede, M.; Hutton, R.; Hoyen, C.; Bonomo, R. A. *Antimicrob. Agents Chemother.* **2000**, *44*, 362–367.
- (21) Otwinowski, Z.; Minor, W. *1997*, *276*, 307–326.
- (22) Winn, M. D.; et al. *Acta Crystallogr., Sect. D: Biol. Crystallogr.* **2011**, *67*, 235–242.
- (23) Emsley, P.; Cowtan, K. *Acta Crystallogr., Sect. D: Biol. Crystallogr.* **2004**, *60*, 2126–2132.
- (24) Schuttelkopf, A. W.; van Aalten, D. M. *Acta Crystallogr., Sect. D: Biol. Crystallogr.* **2004**, *60*, 1355–1363.
- (25) Imtiaz, U.; Billings, E. M.; Knox, J. R.; Mobashery, S. *Biochemistry* **1994**, *33*, 5728–5738.
- (26) Vanhove, M.; Guillaume, G.; Ledent, P.; Richards, J. H.; Pain, R. H.; Frere, J. M. *Biochem. J.* **1997**, *321* (Pt2), 413–417.
- (27) Hermann, J. C.; Pradon, J.; Harvey, J. N.; Mulholland, A. J. *J. Phys. Chem. A* **2009**, *113*, 11984–11994.
- (28) Zafaralla, G.; Manavathu, E. K.; Lerner, S. A.; Mobashery, S. *Biochemistry* **1992**, *31*, 3847–3852.
- (29) Majiduddin, F. K.; Materon, I. C.; Palzkill, T. G. *Int. J. Med. Microbiol.* **2002**, *292*, 127–137.
- (30) Thomas, V. L.; Golemi-Kotra, D.; Kim, C.; Vakulenko, S. B.; Mobashery, S.; Shoichet, B. K. *Biochemistry* **2005**, *44*, 9330–9338.
- (31) Prinarakis, E. E.; Miriagou, V.; Tzelepi, E.; Gazouli, M.; Tzouveleakis, L. S. *Antimicrob. Agents Chemother.* **1997**, *41*, 838–840.
- (32) Dubois, V.; Poirel, L.; Demarthe, F.; Arpin, C.; Coulangue, L.; Minarini, L. A.; Beziau, M. C.; Nordmann, P.; Quentin, C. *Antimicrob. Agents Chemother.* **2008**, *52*, 3792–3794.
- (33) Bret, L.; Chaibi, E. B.; Chanal-Claris, C.; Sirot, D.; Labia, R.; Sirot, J. *Antimicrob. Agents Chemother.* **1997**, *41*, 2547–2549.
- (34) Lobkovsky, E.; Moevs, P. C.; Liu, H.; Zhao, H.; Frere, J. M.; Knox, J. R. *Proc. Natl. Acad. Sci. U.S.A.* **1993**, *90*, 11257–11261.
- (35) Thomson, J. M.; Distler, A. M.; Prati, F.; Bonomo, R. A. *J. Biol. Chem.* **2006**, *281*, 26734–26744.
- (36) Salmeen, A.; Andersen, J. N.; Myers, M. P.; Meng, T. C.; Hinks, J. A.; Tonks, N. K.; Barford, D. *Nature* **2003**, *423*, 769–773.
- (37) van Montfort, R. L.; Congreve, M.; Tisi, D.; Carr, R.; Jhoti, H. *Nature* **2003**, *423*, 773–777.
- (38) Massova, I.; Kollman, P. A. *J. Comput. Chem.* **2002**, *23*, 1559–1576.
- (39) Lamotte-Brasseur, J.; Lounnas, V.; Raquet, X.; Wade, R. C. *Protein Sci.* **2008**, *8*, 404–409.
- (40) Knap, A. K.; Pratt, R. F. *Biochem. J.* **1991**, *273* (Pt1), 85–91.
- (41) Minasov, G.; Wang, X.; Shoichet, B. K. *J. Am. Chem. Soc.* **2002**, *124*, 5333–5340.
- (42) Strynadka, N. C.; Adachi, H.; Jensen, S. E.; Johns, K.; Sielecki, A.; Betzel, C.; Sutoh, K.; James, M. N. *Nature* **1992**, *359*, 700–705.
- (43) Golemi-Kotra, D.; Meroueh, S. O.; Kim, C.; Vakulenko, S. B.; Bulychev, A.; Stemmler, A. J.; Stemmler, T. L.; Mobashery, S. *J. Biol. Chem.* **2004**, *279*, 34665–34673.
- (44) Meroueh, S. O.; Fisher, J. F.; Schlegel, H. B.; Mobashery, S. *J. Am. Chem. Soc.* **2005**, *127*, 15397–15407.
- (45) Krissinel, E.; Henrick, K. *Acta Crystallogr., Sect. D: Biol. Crystallogr.* **2004**, *60*, 2256–2268.
- (46) Kabsch, W. *Acta Crystallogr., Sect. A* **1976**, *32*, 922–923.